The *Dictyostelium* LvsA Protein is Localized on the Contractile Vacuole and is Required for Osmoregulation

Noel J. Gerald, Michael Siano and
Arturo De Lozanne[*]

Section of Molecular Cell & Developmental Biology and
Institute for Cellular and Molecular Biology, University of
Texas at Austin, Austin, TX 78712, USA
* Corresponding author: Arturo De Lozanne,
a.delozanne@mail.utexas.edu

LvsA is a *Dictyostelium* protein that is essential for cytokinesis and that is related to the mammalian beige/LYST family of proteins. To better understand the function of this novel protein family we tagged LvsA with GFP using recombination techniques. GFP-LvsA is primarily associated with the membranes of the contractile vacuole system and it also has a punctate distribution in the cytoplasm. Two markers of the *Dictyostelium* contractile vacuole, the vacuolar proton pump and calmodulin, show extensive colocalization with GFP-LvsA on contractile vacuole membranes. Interestingly, the association of LvsA with contractile vacuole membranes occurs only during the discharge phase of the vacuole. In LvsA mutants the contractile vacuole becomes disorganized and calmodulin dissociates from the contractile vacuole membranes. Consequently, the contractile vacuole is unable to function normally, it can swell but seems unable to discharge and the LvsA mutants become osmosensitive. These results demonstrate that LvsA can associate transiently with the contractile vacuole membrane compartment and that this association is necessary for the function of the contractile vacuole during osmoregulation. This transient association with specific membrane compartments may be a general property of other BEACH-domain containing proteins.

Large volume sphere A (*lvsA*) is a *Dictyostelium* gene that was identified in a genetic screen for cytokinesis mutants (1,2). Analysis of the LvsA predicted amino acid sequence revealed that it is a member of the novel family of BEACH domain-containing proteins. The BEACH domain was named for the beige and Chediak–Higashi syndrome (CHS or LYST) proteins, which were the first that indicated the conserved nature of this motif in mice and humans, respectively (3,4). BEACH domain-containing proteins are found in all organisms from yeast to mammals, but the function of most of these proteins is unknown with the exception of LvsA (cytokinesis), beige/CHS/LYST (lysosomal traffic) and the human protein FAN (sphingomyelinase activation) (2,5,6).

Although the precise function of the BEACH domain is not known, the activity of beige/CHS and FAN in membrane traffic and signaling suggests that these traits may be common among proteins with this domain. In this light, LvsA might also function at a membranous compartment that is required for cytokinesis. It is now clear that membrane traffic plays a crucial role during cytokinesis [reviewed in (7)]. Several trafficking proteins, including clathrin, are required for cytokinesis (8). Interestingly, clathrin and LvsA mutants share several phenotypic characteristics, suggesting that they may participate in the same membrane traffic pathway (2,9). When both mutants attempt cytokinesis they are able to initiate cleavage furrow formation. However, the furrow is not successful and the cells end up with a double furrow morphology that ultimately fails in division. Thus, an LvsA/clathrin-mediated pathway must be required for the proper ingression of the cleavage furrow.

To date, the cellular localization of only one member of the beige family, neurobeachin, has been determined (10). This brain-specific protein is a protein kinase A- anchoring protein found in a compartment closely associated with the Golgi apparatus (10). In addition, a fragment from the mammalian beige-like protein *lba* was shown to localize to vesicles in response to lipopolysaccharide stimulation (11). Biochemical studies have suggested that other beige proteins are cytosolic (2,4). This raises the interesting possibility that beige-related proteins associate with specific membrane compartments in response to a specific stimulus. However, this hypothesis has been difficult to test; given the size of these proteins ($> 400\,kDa$), it is difficult to express recombinant forms tagged with the green fluorescent protein (GFP) or other markers. We show here that we can use genetic recombination to append GFP at the beginning of the LvsA protein to obtain a fully functional product. These studies revealed the transient association of LvsA with an interesting membrane compartment: the contractile vacuole. Remarkably, this association is essential for contractile vacuole function.

Results

GFP-labeling of LvsA by homologous recombination
To label the LvsA protein with GFP, we used homologous recombination to introduce the GFP coding sequence at the 5′ end of the *lvsA* gene. Our construct placed the GFP-LvsA
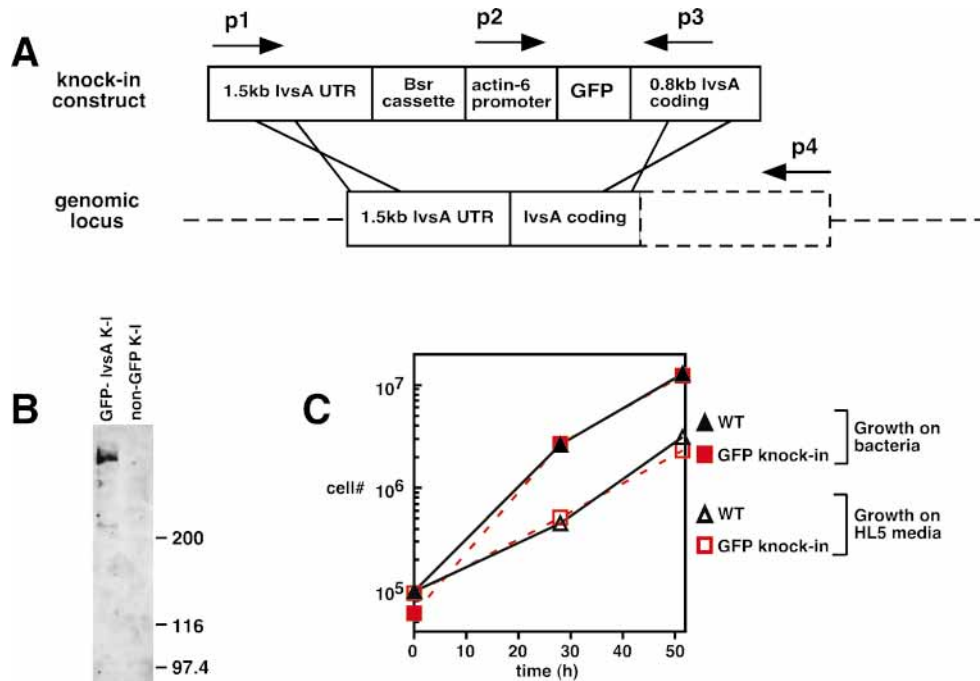
Figure 1: Tagging of the LvsA protein with GFP using a knock-in strategy. (A) Schematic of the construct used to knock-in GFP. Blasticidin was used as a selectable marker for transformation. An identical construct was also created using the actin-6 promoter in front of *LvsA* but without GFP (not shown). Recombinants were screened by PCR with 4 primer combinations (p1, p2, p3, p4). (B) Recombinants express full length GFP-LvsA protein. Western blot using anti-GFP antibody detects a single ~400 kDa band in a cell line that had homologous recombination event with the GFP construct, but not in a recombinant line for the construct lacking GFP. (C) GFP-LvsA is functional in cytokinesis. Wild-type cells and knock-in cell lines were grown in shaking suspension culture on bacteria or in HL5 nutrient media. In both cases, knock-in cell lines grew at rates identical to wild type, demonstrating that GFP-LvsA is functional in cytokinesis.
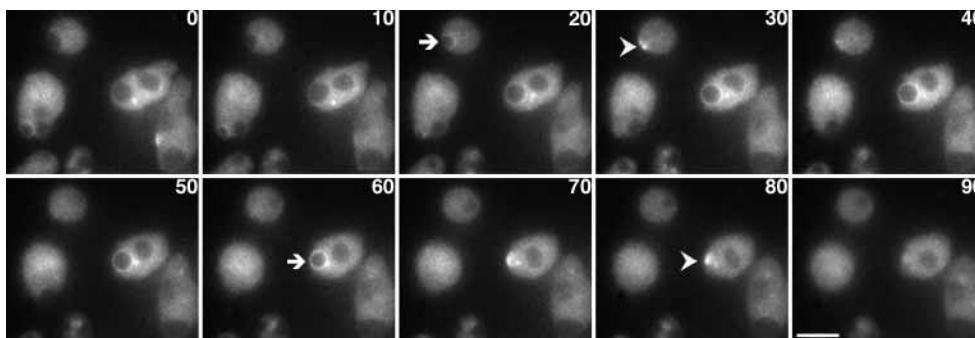

Figure 2: GFP-LvsA is localized on the contractile vacuole. Time-lapse imaging of cells expressing GFP-LvsA . Cells were incubated in dH$_2$O and epifluorescence images (100 ms exposure) were taken every 5 s. GFP-LvsA was clearly visible outlining the contractile vacuoles that lacked internal fluorescence (arrows). These compartments gradually expanded and contracted to a small spot that persisted after contraction (arrowheads). GFP-LvsA is also found in the cytoplasm. Numbers indicate time elapsed in seconds. Scale bar = 10 μm. Movies are available through the Traffic web page (www.traffic.dk) in the video gallery at http://www.blackwellmunksgaard.dk/tidsskrifter.nsf/tidsskrifter/Traffic/videogallery?OpenDocument.

fusion protein under the control of the actin-6 promoter (Figure 1A). We also designed a similar construct without GFP as a control for possible effects of either GFP or the actin-6 promoter on the activity of LvsA. We introduced these constructs into wild-type *Dictyostelium* cells (strain DH1) and screened for successful recombination events by PCR.

Western blot analysis with an anti-GFP antibody detected a single GFP-tagged product of the predicted size (>400 kDa) only in the lines transformed with the GFP-knock-in construct (Figure 1B). Similar Western blot analysis with an anti-LvsA antibody indicated that the GFP-tagged protein was expressed at levels similar to those of LvsA found in wild-type

cells. To determine whether this GFP-LvsA fusion protein was functional, cells were assessed for their ability to divide in suspension cultures. LvsA mutant cells are not able to grow in these conditions due to their cytokinesis defect (2). All cell lines grew at rates identical to wild-type cells, indicating that the GFP did not disrupt LvsA function for growth in suspension (Figure 1C).

GFP-LvsA is localized on the contractile vacuole network

The distribution of GFP-LvsA in living cells was observed by epifluorescence microscopy. We found that the overall fluorescence of GFP-LvsA was largely diffuse throughout the cytoplasm with occasional punctate structures visible in the cytoplasm. However, when cells were placed in hypoosmotic conditions, GFP-LvsA was readily visible on large contracting vesicles (Figure 2, arrows) (see QuickTime Movies[1]). After vesicle contraction, GFP-LvsA fluorescence remained visible for a few seconds as a distinct spot (Figure 2, arrowheads). These observations suggested that LvsA localizes to the contractile vacuole membrane.

To confirm these observations, we determined the localization of GFP-LvsA in comparison with known markers of the contractile vacuole. However, since the GFP signal was not visible in our fixed preparations, we used an anti-GFP antibody for immunofluorescence microscopy. This antibody provided a very strong signal with minimal background and displayed staining that was similar to the distribution of GFP-LvsA seen in live cells. In these fixed samples, the diffuse cytoplasmic distribution of GFP-LvsA was not visible, which we interpret as soluble protein extracted during fixation. GFP-LvsA immunofluorescence was punctate throughout the cytoplasm (Figure 3, arrowheads) and was also prominent on large vacuoles (Figure 3, arrows). In addition, GFP-LvsA appeared to decorate thin branching structures radiating from the stained vacuoles. No significant GFP-LvsA localization was observed at the cleavage furrows of dividing cells (Figure 3C–D).

The observation that the GFP-LvsA-stained vesicles contract when living cells are placed in hypoosmotic conditions suggested that these compartments were elements of the contractile vacuole. In addition, the GFP-LvsA-stained structures revealed by immunofluorescence resembled the tubules and cisternae of the contractile vacuole (CV) system (12). To confirm that these structures are indeed elements of the CV, GFP-LvsA cells were fixed and prepared for double label immunofluorescence. Vacuolar proton pump (V-H$^+$ATPase) and calmodulin were used as markers for the CV (12).

In wild-type cells, V-H$^+$ATPase localizes to membranes of the endolysosomal system and also strongly localizes to
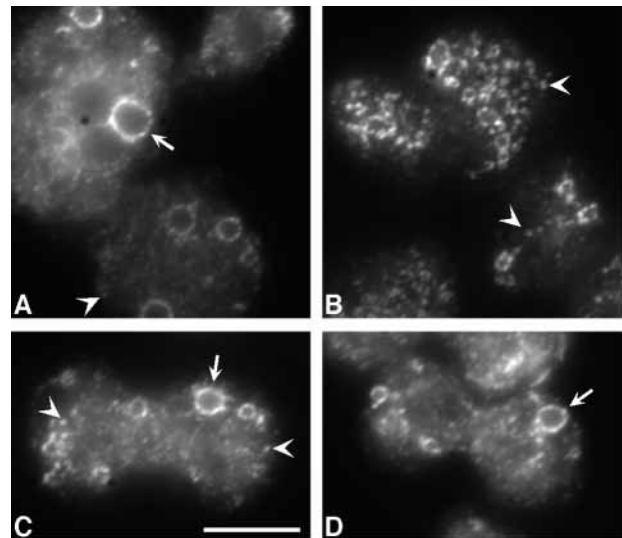
Figure 3: Immunofluorescence localization of GFP-LvsA. GFP-LvsA cells were fixed and stained with an anti-GFP antibody and an FITC conjugated secondary antibody. GFP-LvsA is distributed throughout the cytoplasm with a punctate appearance (arrowheads) and on the large contractile vacuole (arrows). In addition, GFP-LvsA also decorates reticular structures that radiate from the contractile vacuoles (see Figure 5). Panels A and B show cells in interphase. Cells in B are imaged at a focal plane close to the substrate. Panels C and D depict two cells in cytokinesis. GFP-LvsA was not concentrated in the region of the cleavage furrow. Scale bar = 10 μm.

membranes of the contractile vacuole (12). Under the proper fixation conditions, V-H$^+$ATPase outlines the large cisternae of the contractile vacuole (Figure 4A, arrowhead) and the fine branchwork of ducts and tubules that connect these cisternae (Figure 4D, arrowheads). GFP-LvsA also stained the same tubular and vacuolar structures of the cell (Figure 4B,E, arrowheads). Although the two stains overlapped considerably, colocalization of these markers was not complete along the entire CV structure; GFP-LvsA was absent from some portions of the CV tubular network (Figure 4F, arrow). Furthermore, the V-H$^+$ATPase stained prominently a membranous compartment closely associated with the nucleus while GFP-LvsA did not (Figure 4C, arrow). This membranous compartment probably represents the endolysosomal system, which is known to be populated by the V-H$^+$ATPase (13). Conversely, much of the punctate cytoplasmic GFP-LvsA staining did not stain with V-H$^+$ATPase (Figure 4C,F, arrowheads).

As reported in the literature, calmodulin localizes almost exclusively to contractile vacuole tubules and cisternae in fixed cells (14). GFP-LvsA and calmodulin localized to the same vacuolar and tubular structures in the cell (Figure 5, arrows). As with V-H$^+$ATPase staining, GFP-LvsA did not overlap calmodulin staining throughout the entire CV network, and calmodulin did not colocalize with the punctate cytoplasmic GFP-LvsA distribution (Figure 5, arrowheads).
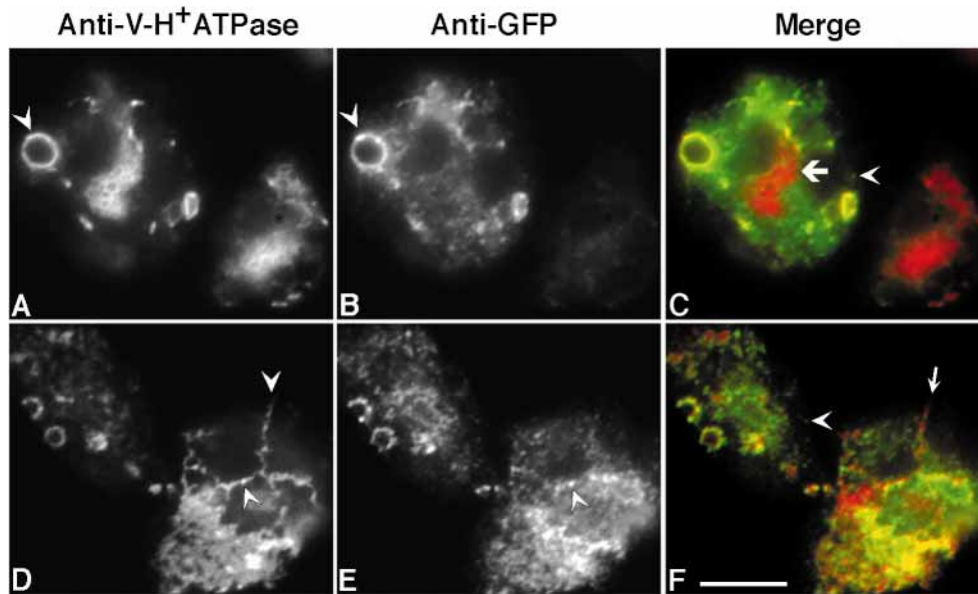
Figure 4: GFP-LvsA colocalizes with the V-H+ATPase on the contractile vacuole. GFP-LvsA-expressing cells were fixed and stained for both V-H+ATPase (red) and GFP (green). V-H+ATPase is localized to the cisternae and tubular reticulae of the contractile vacuole network (panels A and D, arrowheads). GFP-LvsA also localizes to these structures (panels B and E, arrowheads). The distribution of LvsA on the tubular networks is not as extensive as that of the V-H+ATPase (panel F, arrow). Some structures labeled by V-H+ATPase stain were not labeled by the GFP-LvsA stain (panel C, arrows). These may be components of the endolysosomal system. Similarly, the punctate cytoplasmic distribution of GFP-LvsA did not overlap with the V-H+ATPase distribution (panel C and F, arrowheads). Scale bar = 10 μm.
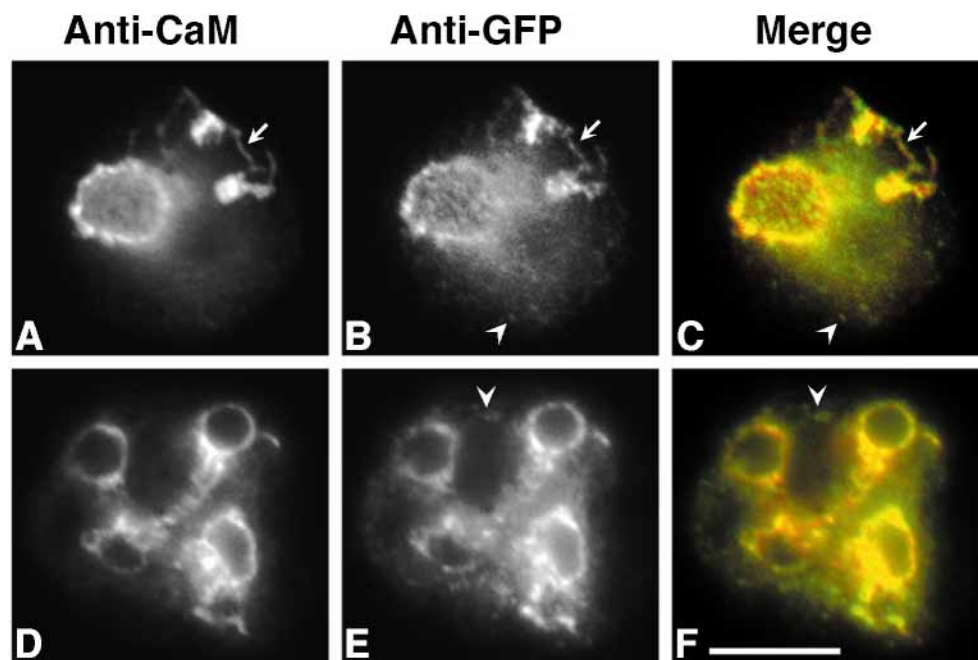

Figure 5: GFP-LvsA colocalizes with calmodulin on the contractile vacuole. GFP-LvsA cells were fixed and double stained for both GFP and calmodulin. Calmodulin localizes to the tubules (arrows) and vacuoles of the contractile vacuole network (panels A and D). GFP-LvsA shows considerable overlap at these structures (panels B and E). The punctate cytoplasmic distribution of GFP-LvsA does not colocalize with the calmodulin distribution (panels B, C, E and F, arrowheads). Scale bar = 10 μm.

These results confirmed that GFP-LvsA localizes to elements of the contractile vacuole in addition to a punctate distribution in the cytosol.

LvsA⁻ mutant cells have osmoregulation defects

The localization of LvsA to the contractile vacuole suggested that it might play a role in the function of this organelle. To test this possibility, wild-type and *lvsA⁻* cells [strain AD 60 (2)] were placed in distilled water to monitor their reaction to hypo-osmotic stress. After 50 min in water, wild-type cells were slightly swollen, but still retained the ability to crawl and change shape (Figure 6, upper panels). In contrast, *lvsA⁻* cells swelled into complete spheres that had difficulty making cellular extensions or remaining attached to the coverslip (Figure 6, lower panels).

To observe the osmoregulation defect in more detail, adherent cells were flattened slightly by agar overlay. Wild-type cells under these conditions were able to crawl readily. Upon the addition of hypo-osmotic medium, wild-type CV's were visible as phase lucent compartments that gradually filled and then swiftly contracted in 3–4 s (Figure 7A) (see QuickTime Movies). After successful discharge, additional phase lucent vacuoles filled to repeat the cycle.

Mutant *lvsA⁻* cells under hypoosmotic stress contained several swollen phase lucent vacuoles (see QuickTime Movies). However, most of these vacuoles showed no size changes or evidence of discharge for periods of observation up to 30 min (Figure 7B). Occasionally, two types of intermittent vacuole discharge events were observed i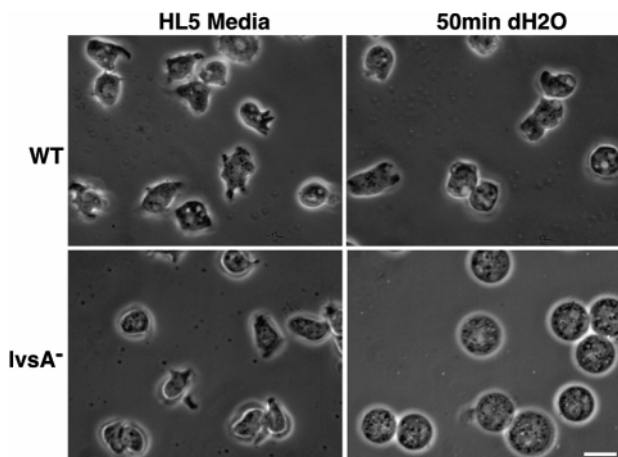n mutant cells (Figure 7C,D). One type of mutant vacuole discharge resembled wild-type discharge as the phase lucent vacuoles contracted within 3–4 s (Figure 7C, arrows). In the second type of mutant discharge, vacuoles appeared to fuse suddenly with the surface of the cell and a bleb formed at the same site, suggesting rapid addition of new membrane (Figure 7C,D, triangular arrows). This is reminiscent of the abnormal vacuole fusion events previously reported in the drainin null mutant; a cell line that is defective in controlled vacuole-plasma membrane fusion (15). Both types of vacuole discharge that we observed were infrequent, and were not followed by the appearance of new vacuoles. For example, the vacuoles that discharged in Figure 7(C) (time frames 2, 22 and 33 s) did not re-appear later.

The association of GFP-LvsA with the CV is transient

Our observations suggested that the contractile vacuoles of *lvsA⁻* mutants can swell but are unable to discharge effectively. This prompted us to look more closely at the distribution of GFP-LvsA during contractile vacuole activity in wild-type cells. Interestingly, we found that the contractile vacuole does not appear to be labeled by GFP-LvsA as it is expanding in volume (Figure 8, arrowhead at 0 and 10 s) (see QuickTime Movies). Later, the vacuole becomes prominently labeled by GFP-LvsA and the discharge phase ensues (Figure 8, arrowhead at 20–60 s). GFP-LvsA remains associated with the vacuolar membranes throughout the discharge phase until it is reduced to a very bright spot (Figure 8, arrowhead at 70–80 s). The fluorescence of GFP-LvsA quickly dissipates from that spot (Figure 8, arrowhead at 90 s) and the contractile vacuole that subsequently begins to reform does not show any signs of labeling until the following discharge (Figure 8, arrowhead at 290 s). This transient association with the CV differs from the distribution of drainin which remains associated with the CV during both expansion and discharge phases (15).

LvsA⁻ cells have contractile vacuole structural defects

To understand in better detail the basis of the contractile vacuole defect in the absence of LvsA, we determined the distribution of the contractile vacuole markers described above in *lvsA⁻* mutant cells. Interestingly, *lvsA⁻* mutant cells stained for V-H⁺ATPase showed an extensive rearrangement of contractile vacuole membranes. In contrast to wild-type cells, mutant cells showed multiple vacuoles that were often clumped together in the cell. Many small vesicular elements were visible in mutant cells, while the branching networks of tubules and ducts of wild-type cells were absent (Figure 9).

Most remarkably, the distribution of calmodulin was drastically changed by the loss of LvsA. We found that a large portion of calmodulin staining in *lvsA⁻* mutant cells was diffuse throughout the cytoplasm (Figure 10). Occasional punctate structures were also labeled by calmodulin. However, none of the vesicular elements highlighted by V-H⁺ATPase were observed with calmodulin staining. This

Figure 6: *LvsA* mutant cells are impaired in osmoregulation. *LvsA⁻* mutant cells were allowed to attach to coverslips in nutrient medium. The medium was exchanged for dH₂O and the cells were re-examined after 50 min Wild-type cells (WT) were partially swelled under the hypo-osmotic load, but were still able to crawl and change shape. *LvsA⁻* cells were completely swelled in dH₂O and barely remained attached to the coverslip. However, a few *lvsA⁻* cells lysed after 50 min of this treatment, suggesting that the mutants retain some low level of osmoregulation. Scale bar = 10 μm.
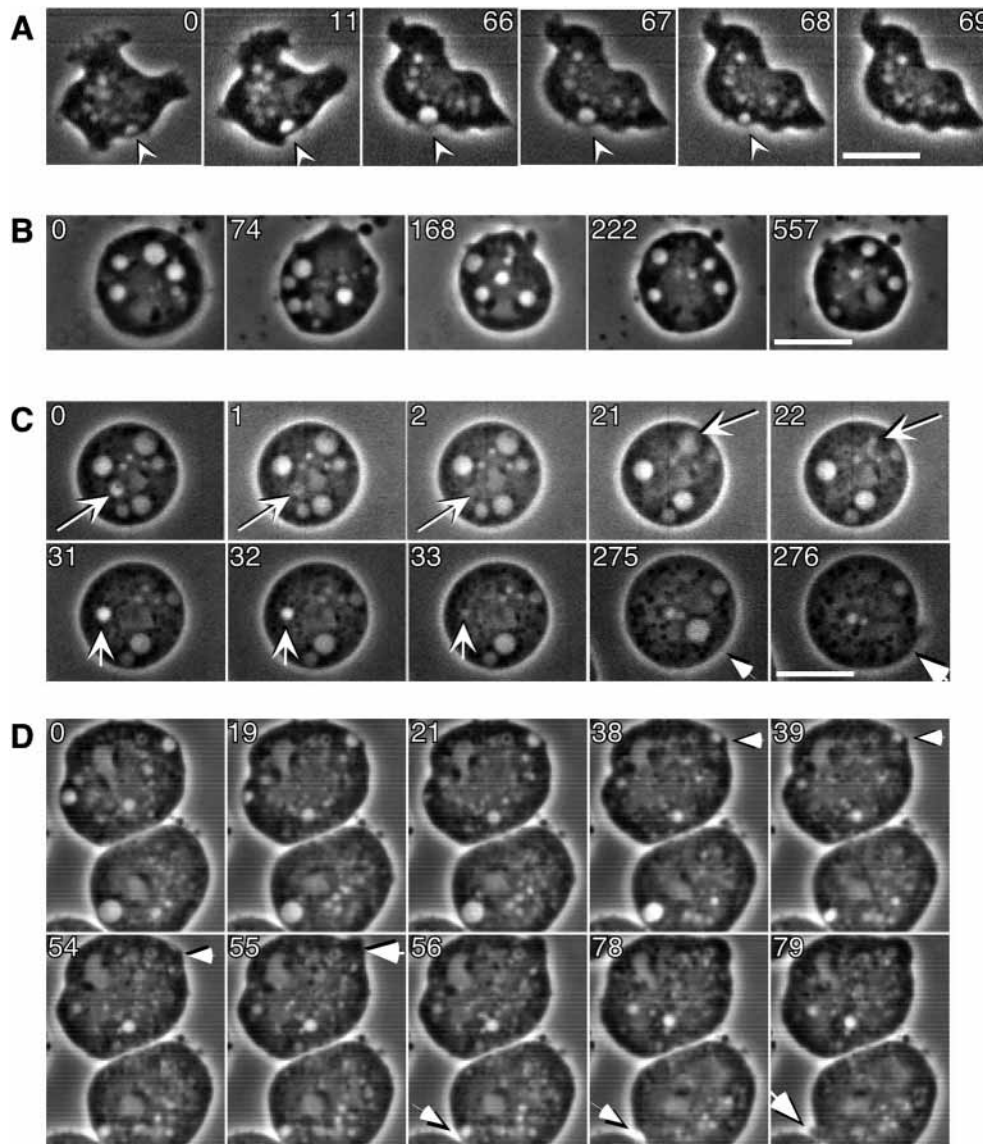
Figure 7: The contractile vacuoles of *LvsA* mutant cells are not able to expel water efficiently. Cells were flattened with agar overlay under dH$_2$O, and observed by low-light microscopy. (A) Wild-type cells show rapid filling and discharging of contractile vacuoles (arrowheads). (B) Most *lvsA$^-$* cells contain phase lucent vacuoles that do not discharge. (C) A few *lvsA$^-$* cells discharge vacuoles in a manner similar to wild-type cells (arrows). However, vacuoles sometimes fused suddenly to the plasma membrane producing a slight bleb (triangle arrows). (D) Two more examples of *lvsA$^-$* cells with vacuole fusion to the plasma membrane. The vacuoles constrict down to smaller-sized vesicles that vanish with the appearance of blebs (arrows). Numbers indicate the time elapsed in seconds. Scale bar = 10 µm. Movies are available through the Traffic web page (www.traffic.dk) in the video gallery at http://www.blackwellmunksgaard.dk/tidsskrifter.nsf/tidsskrifter/Traffic/videogallery?OpenDocument

suggests that calmodulin is not associated with the CV membrane elements in the absence of LvsA.

Discussion

In this study, we tagged and localized GFP-LvsA in an effort to elucidate the function of this novel BEACH domain-containing protein. To tag LvsA with GFP, we used a knock-in approach to insert GFP and an actin promoter in front of the LvsA-coding region. This approach has the advantages that we did not have to construct a very large expression vector and that the fusion protein is expressed from its native locus in the genome. The resulting cells express wild-type levels of GFP-tagged LvsA (data not shown) and have a wild-type phenotype.

We found that in living cells, the majority of GFP-LvsA fluorescence appears to be cytosolic with some punctate localization throughout the cytoplasm. GFP-LvsA is also
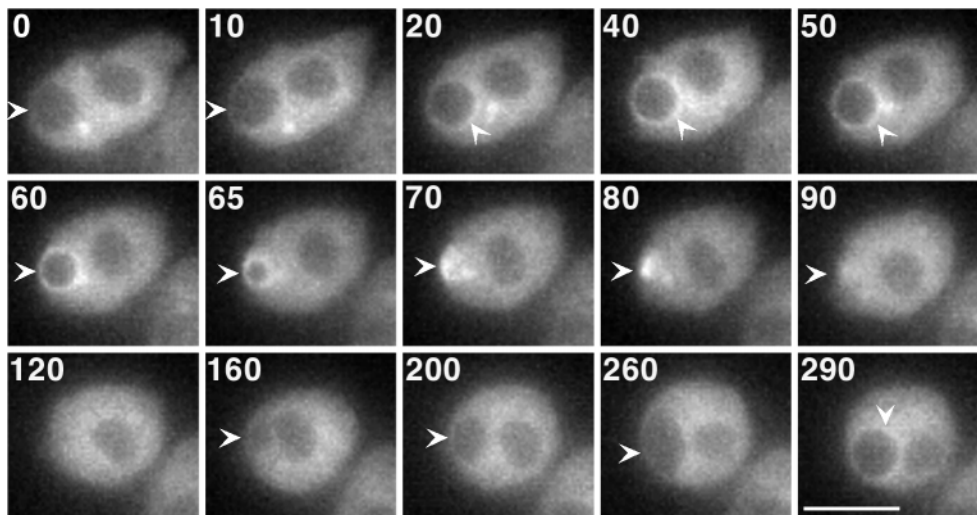
Figure 8: GFP-LvsA associates with the membrane of the contractile vacuole only during the discharge phase. One of the cells in Figure 2 is magnified here. Notice how in the first two-time frames there is no discernible labeling of the contractile vacuole by GFP-LvsA above the level of the cytoplasmic background. Beginning at 20 s, GFP-LvsA begins to clearly label the contractile vacuole, which then starts to contract at 50 s. Contraction is complete by 80 s, when the contractile vacuole is visible as a bright spot of GFP-LvsA fluorescence. At 130 s, the contractile vacuole begins to expand again and continues to expand until 280 s. Throughout this time, the vacuole is not labeled by GFP-LvsA . At 290 s, the vacuole becomes marked by GFP-LvsA for a new cycle of contraction. Scale bar = 10 μm. Movies are available through the Traffic web page (www.traffic.dk) in the video gallery at http://www.blackwellmunksgaard.dk/tidsskrifter.nsf/tidsskrifter/Traffic/videogallery?OpenDocument
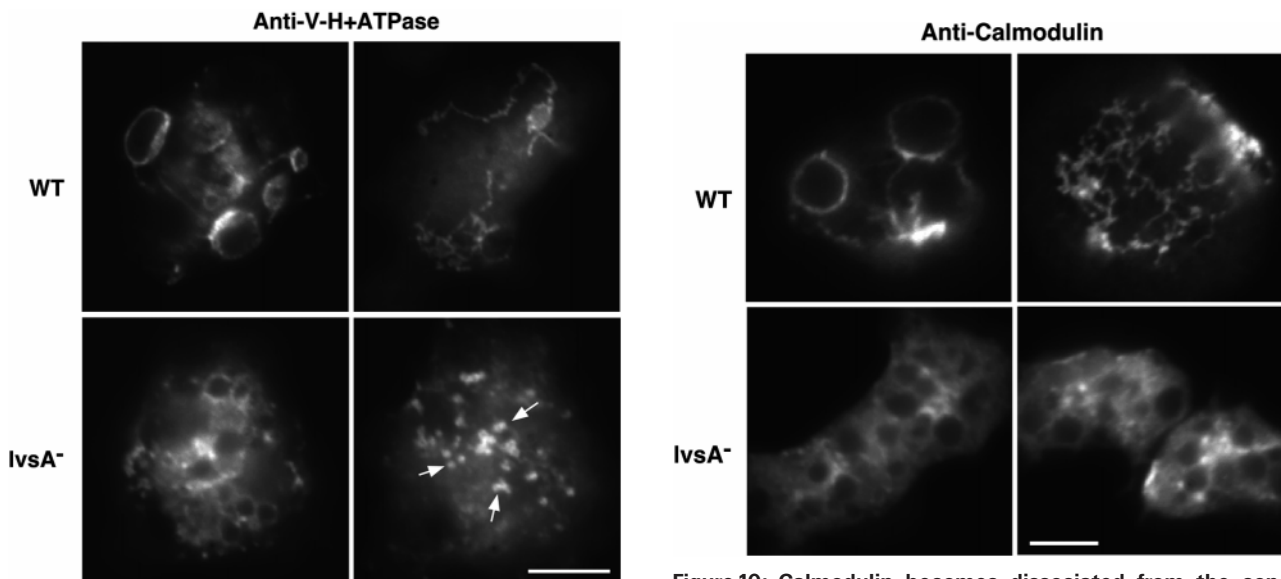

Figure 9: Loss of LvsA causes abnormal contractile vacuole formation. Wild-type and *lvsA*⁻ cells were fixed and stained with an anti-V-H+ATPase antibody. Upper panels show two wild-type (WT) cells that display the normal structure of the contractile vacuole of large vesicles and network of tubules and sacs. Lower panels depict 2 focal planes of a representative LvsA mutant cell. Mutant cells display multiple vacuolar compartments clumped together. The characteristic long reticular elements were not observed in mutants. Instead, small vesicular structures were visible close to the substrate where contractile vacuole reticulae would normally be expected (arrows). Scale bar = 10 μm.

Figure 10: Calmodulin becomes dissociated from the contractile vacuole in the absence of LvsA. Wild-type and *lvsA*⁻ cells were fixed and stained with an anti-calmodulin antibody. Upper panels show two wild-type (WT) cells that show the association of calmodulin with the membranes of the contractile vacuole network. Vacuoles and tubules are prominently labeled and there is little staining in the cytoplasm. In contrast, the lower panels illustrate the distribution of calmodulin in *lvsA*⁻ cells. In these cells calmodulin staining is mostly diffuse throughout the cytoplasm. Some punctate structures are also visible. None of the abnormal contractile vacuole structures (see Figure 9) in these cells were stained by calmodulin. Scale bar = 10 μm.

prominent on the cisternae of the CV as they contract and discharge. GFP-LvsA localization at these vacuoles seems brightest at the end of the contraction phase, and the resulting spot of fluorescence often lingers for a few seconds after the discharge. Similar observations have been made in other studies focused on the CV (12,15–17). This pattern of fluorescence is expected for CV-associated molecules, as the vacuoles are thought to become highly folded when they discharge.

To confirm that GFP-LvsA was associated with membranes of the contractile vacuole system, we examined its colocalization with two markers for the CV: calmodulin and V-H$^+$ATPase. GFP-LvsA overlaps extensively with both markers on the cisternae and tubular extensions of the CV. However, GFP-LvsA is clearly found in punctate cytoplasmic structures that do not stain with calmodulin or V-H$^+$ATPase. We interpret these to be a population of vesicles that are distinct from the CV and the endolysosomal system, since they do not stain with V-H$^+$ATPase. The identity and function of these vesicles remains to be determined.

LvsA$^-$ cells have defects in contractile vacuole function

Since GFP-LvsA localizes to components of the contractile vacuole, it is not surprising that lvsA$^-$ cells have defects in the function of this organelle. Unlike wild-type cells, lvsA$^-$ cells swell when placed in hypo-osmotic conditions. Large vacuoles can still form in lvsA$^-$ mutants when they are first in contact with water. However, the discharge of those vacuoles is often abnormal in that they appear to fuse entirely with the plasma membrane. Although this is similar to the vacuolar discharge defect of drainin null mutants (15), LvsA is likely to act at a different step in the discharge pathway. LvsA$^-$ mutants do not produce the massive singular vacuoles seen in drainin null mutants. In addition to discharge defects, lvsA$^-$ mutants fill vacuoles erratically. While multiple large vacuoles can be observed in lvsA$^-$ mutant cells, these large vacuoles are not readily replaced when an occasional discharge event does occur. Thus, LvsA appears to be important during the discharge and recovery phases of CV function.

The lvsA$^-$ contractile vacuole defect is also apparent in the distribution of molecular markers for the CV. V-H$^+$ATPase immunofluorescence shows that the structure of the CV is abnormal in lvsA$^-$ cells. Irregular vacuoles are often clumped together and the long reticular tubular elements between vacuoles are not apparent. In addition, there are areas of abnormal V-H$^+$ATPase staining close to the plasma membrane.

Surprisingly, calmodulin becomes dissociated from all CV structures in lvsA$^-$ cells and appears mostly dispersed in the cytoplasm. Although the function of calmodulin at the CV is not known, its mislocalization could explain the defects in contractile vacuole activity.

The association of calmodulin with the membranes of the CV is not disrupted in most other known CV mutants. In drainin mutants, both V-H$^+$ATPase and calmodulin markers decorate the immense defective vacuoles (15). In rabD mutants, both V-H$^+$ATPase and calmodulin markers are also colocalized, and decorate a clump of material next to the plasma membrane (18). Intriguingly, the mutant that also displays diffuse calmodulin staining is the clathrin null cell. Clathrin null cells are also known to have CV defects (19). In clathrin null cells, the large cisternae of the CV appear to be completely absent by electron microscopy. V-H$^+$ATPase in these cells is found in many small vesicles and calmodulin does not colocalize with the V-H$^+$ATPase staining, but remains diffuse, similar to lvsA$^-$ mutants (M. Clarke and T. O'Halloran, personal communication). This similarity is intriguing in light of all their common phenotypes: both are osmosensitive, calmodulin is dissociated from the contractile vacuole, and they fail in cytokinesis due to similar cleavage furrow ingression defects (9). These observations suggest that clathrin and LvsA participate at different steps of the trafficking pathways that are essential for those cellular functions. We postulate that clathrin is involved at an early step in the biogenesis of the CV, whereas LvsA is required for CV discharge.

The role of LvsA in contractile vacuole function

The osmoregulatory defect of lvsA$^-$ mutants shows that LvsA plays an important role in CV function. This role appears to be important for only the discharge phase but not for the swelling phase of the CV. This possibility is supported by the observation that the CVs in wild-type cells are labeled by GFP-LvsA only as they discharge and not as they swell. Moreover, the CVs of lvsA$^-$ cells are able to swell initially but fail to discharge normally.

Two models have been postulated to explain the contractile activity of the CV. One model suggests that unconventional myosin motors contribute the contractile force necessary for water discharge (16,20). It has also been suggested that calmodulin may interact with those motors to regulate their activity (14,16). Since LvsA is required for the recruitment of calmodulin to the CV membrane, it may be possible that the discharge defect of lvsA$^-$ cells is due to their inability to activate the contractile apparatus. An objection to this model is that none of the tested Dictyostelium myosin mutants display any contractile vacuole defects (21). Nonetheless, calmodulin probably plays an important role in CV function and the dissociation of calmodulin from CV membranes is a likely cause of CV dysfunction in lvsA$^-$ cells.

A second model of CV discharge proposes that changes in membrane tension drive the rounding of the CV and water discharge (22). In this view an increase in the spontaneous curvature of the membrane bilayer of the CV generates enough tension to force the expulsion of water. One potential mechanism to change the spontaneous curvature of a membrane is by asymmetrically changing the lipid

composition of the membrane bilayer leaflets (23). This suggests a possible role for LvsA. FAN, a mammalian protein related to LvsA, is a known activator of a neutral sphingomyelinase (6). Cleavage of sphingomyelin on one side of a membrane has been shown dramatically change the membrane's curvature (24). Thus, it is feasible that LvsA may activate a specific pathway that may alter the lipid composition of the CV to induce membrane tension and water discharge.

The role of LvsA in cytokinesis

Both *lvsA*⁻ and clathrin-null mutants have a cytokinesis defect. When these cells are cultured in suspension, they form a cleavage furrow that does not divide the cell (2,9). Instead, this furrow eventually partitions into two separate constrictions. The contraction of these two furrows causes the equator to bulge out between them. Eventually, both furrows regress and the cell rounds up to become multinucleate. At present, the exact cause of this peculiar defect is unknown. However, it is likely that their requirement for cytokinesis is not direct, since neither LvsA (Figure 3) nor clathrin (25) localizes to the cleavage furrow during cell division.

It may seem possible that the cytokinesis defect of *lvsA*⁻ and clathrin mutants is directly related to the dysfunction of their contractile vacuoles. This organelle fragments into small vesicles when cells enter mitosis and reassembles as cells initiate cytokinesis (14,17). Subsequently, the CV displays extensive activity during cleavage furrow ingression (26). However, contractile vacuole activity is unlikely to be essential for cytokinesis, since other *Dictyostelium* CV mutants do not have cytokinesis defects (15,18).

The mislocalization of calmodulin in both *lvsA*⁻ and clathrin null mutants suggests a common mechanism for cytokinesis failure in these two cells. Calmodulin is required for cytokinesis in *Dictyostelium* (27) and also seems to play a direct role at the cleavage furrow in vertebrate cells. Calmodulin localizes to the equatorial cortex before constriction and gains intensity at the furrow throughout cytokinesis (28–30). Interestingly, disruption of calcium signaling in Xenopus eggs leads to the formation of one or two eccentric furrows that fail to constrict to completion (30). This phenotype may be related to the cytokinesis failure of clathrin and *lvsA*⁻ mutant cells.

Finally, it is possible that the cytokinesis defect of *lvsA*⁻ is not associated at all with the osmoregulatory defects. In addition to the CV, LvsA is also found as a punctate distribution throughout the cytoplasm. It is feasible that LvsA plays a critical role for cytokinesis at a location different from the CV. It remains to be tested whether these two roles of LvsA are in fact distinct and separable.

Materials and Methods

Cell culture

For most experiments, cells were grown on Petri dishes with HL5 medium (31) supplemented with 60 U/ml penicillin and 60 μg/ml streptomycin. Cells

that carried the green fluorescent protein (GFP)-myosin II expression vector (32) were grown in medium supplemented with 10 μg/ml G418. Cells expressing GFP-LvsA (see below) were grown in medium supplemented with 10 μg/ml Blasticidin S. *LvsA* mutant strain AD-60 was described previously (2).

Tagging LvsA with GFP by homologous recombination.

Since our attempts to localize LvsA by immunofluorescence with anti-LvsA antibodies were unsuccessful, we decided to tag LvsA with GFP to follow the distribution of the fusion protein. However, cloning of the entire *lvsA*-coding region into our expression vectors was unwieldy given the large size (> 11 kb long) of the *lvsA* gene. To circumvent this problem, we designed a construct to introduce the GFP sequence at the 5′ end of the *lvsA* gene by homologous recombination (Figure 1A). In this 'knock-in' construct, the GFP coding sequence was fused in frame with the first 0.8 kb of the *lvsA* open reading frame. The GFP-fusion construct was placed under the control of the *Dictyostelium* actin-6 promoter. The construct also contained 1.5 kb of 5′ *lvsA* untranslated sequences used to target the construct. A blasticidin-resistance cassette was included as the selectable marker. A second construct was also created that did not contain GFP, but placed the actin 6 promoter directly in front of the *lvsA* reading frame. This control construct was designed to test whether GFP disturbed the normal function of LvsA. In all other aspects, the two 'knock-in' constructs were the same. Homologous recombination of these constructs into the locus of the *lvsA* gene in wild-type cells should lead to the replacement of the lvsA promoter by the actin-6 promoter ± GFP fusion construct.

Linearized constructs were introduced into wild-type (DH1 and NC4A2) cells by electroporation, and clonal populations were selected in 96-well plates in HL5 medium containing 10 μg/ml blasticidin. Colonies were screened by Western blot analysis with an anti-GFP antibody or by the polymerase chain reaction (PCR). We used two primer pairs (P1/P3 and P2/P4, Figure 1A) designed to test for the double cross-over recombination of the constructs into the *lvsA* locus. In wild-type cells, the P1/P3 pair yields a band of 715 bp but not the P2/P4 pair. After recombination, the P1/P3 pair fails to yield a product and the P2/P4 pair yields a 1957-bp product.

For confirmation of gene expression, *Dictyostelium* whole-cell lysates (1 × 10⁶ cells/lane) were prepared as described (33) and separated on a 7.5% low-bis-acrylamide SDS PAGE as described (34). The gel was blotted onto nitrocellulose and probed with a 1 : 1000 dilution of a polyclonal anti-GFP antibody kindly provided by Dr Dan Kiehart (35) or a polyclonal anti-GFP antibody raised in our own laboratory. The blot was developed with an HRP-conjugated goat anti-rabbit secondary antibody and ECL detection kit (Pierce, Rockford, IL, USA). To assess the relative level of expression of GFP-LvsA in comparison to that found in unlabeled wild-type cells we processed a duplicate blot with antibodies raised against the C-terminus of LvsA (2). This analysis demonstrated that in one cell line, NG-190, GFP-LvsA was expressed at the same level as wild-type LvsA. Another cell line, MS-2H10, expressed GFP-LvsA to a level about two-fold higher than unlabeled LvsA. No cell line was found with higher overexpression of GFP-LvsA .

Live observation of GFP-LvsA

Cells expressing GFP-LvsA were allowed to adhere to #1 coverslip-chambers (Nalge-Nunc Int., Naperville, IL, USA) and were incubated in dH₂O to reduce autofluorescence from the medium, and to induce the activity of the contractile vacuole. Cells were imaged on an inverted Nikon Microscope TE200 (Nikon Instruments, Dallas, TX, USA) equipped with a 100 × 1.4 NA PlanFluor Objective, shuttered illumination, and a Quantix 57 camera (Roper Scientific, Tucson, AZ, USA) controlled by Metamorph (Universal Imaging Corp., West Chester, PA, USA). Images were taken with

a binning setting of 1×1 or 2×2. Epifluorescence illumination was shuttered at 100 ms and the interval between acquisitions was 5 s.

Anti-GFP immunofluorescence

GFP-LvsA could not be detected by its own fluorescence under any fixation conditions. To circumvent this difficulty, the polyclonal anti-GFP antibody that recognized a single band in Western Blots was used for immunofluorescence. Adherent cells on coverslips were fixed for 5 min in $-15\,°C$ methanol and washed in phosphate-buffered saline. The coverslips were incubated for 45 min in block solution (0.5% bovine serum albumin, 0.045% fish gelatin, 0.02% sodium azide in PBS), and then incubated for 1 h with anti-GFP antibody diluted 1 : 1000 in 5% BSA in TBS. After four 5-min washes in block solution, the coverslips were incubated for 1 h with FITC-conjugated goat anti-rabbit antibodies diluted 1 : 500 in block solution. Subsequently, coverslips were washed, mounted, and viewed by epifluorescence on a Zeiss Axioplan (Oberkochen, Germany) microscope equipped with a 1.3-NA $100\times$ oil objective. Images were obtained with a Star I Photometrics (Tucson, AZ, USA) cooled charge-coupled device camera using IPlab software (Signal Analytics, Vienna, VA, USA). Adobe Photoshop 5.0 (San Jose, CA, USA) was used to adjust the contrast of the digital images. The Photoshop unsharp mask filter was also applied to differential interference contrast (DIC) images.

To confirm the specificity of the GFP staining we fixed and stained wild-type cells that lacked GFP. No background signal was observed in these cells.

For double-label experiments with contractile vacuole markers, a modified fixation protocol was used (12). Briefly, adherent cells on coverslips were incubated 15 min in 1/3 strength HL5 medium to enhance activity of the contractile vacuole. Cells were then fixed in 2% formaldehyde, 0.1% DMSO in 1/3 strength HL5 for 5 min, and subsequently placed in $-15\,°C$ methanol, 1% formaldehyde for 5 min. Cells were washed and blocked as described above. Antibodies for contractile vacuole markers were a generous gift from Margaret Clarke. For localization of proton pumps, a monoclonal antibody raised against the 100 kDa integral membrane subunit of vacuolar-H^+ATPase (N2) (36), was used at 1 : 40 dilution. For localization of calmodulin, monoclonal antibody 2D1 was used at 1 : 20 dilution. Secondary antibodies in double-label experiments were incubated on coverslips simultaneously for 1 h. Fluorescein-labelled goat anti-mouse secondary antibodies at 1 : 50 were used to detect mouse primary antibodies for vacuolar markers and rhodamine-labeled goat anti-rabbit antibodies were used at 1 : 50 to detect rabbit anti-GFP primary antibody. Coverslips were washed, mounted and viewed as described above.

Osmoregulation assay

Wild-type or mutant cells were allowed to attach to coverslips in HL5 medium. Vacuum grease was used to line parallel sides of the coverslips that were then inverted on glass slides to create simple flow-through chambers. A field of cells in HL5 was imaged on the Zeiss Axioplan microscope described above with a 100×1.3NA phase-contrast objective. Next, the media was exchanged with a few volumes of dH_2O and allowed to sit for 50 min with periodic dH_2O perfusion to prevent anoxia. At the end of this time period, a second image was taken on the same field.

Observation of contractile vacuole dynamics

Wild-type or mutant cells were allowed to attach to coverslips in HL5. For viewing the contractile vacuole, the medium was replaced with dH_2O for approximately 5 min, and agar-overlay was assembled on top of the cells. Vacuum grease runners were lined on either side of the agar-overlay, and the coverslips were inverted onto glass slides as before. The extent of cell compression under agar was directly related to 'wicking' of fluid from the space in the chamber. Additional water was perfused periodically.

Since the contractile vacuole is extremely sensitive to light toxicity (12), the light source was turned to its lowest setting and a neutral density filter was used in combination with a 600-nm red filter so that no image was visible through the eyepieces. A 100×1.3NA phase contrast objective was used on the Zeiss Axioplan. Images were acquired at 1-s intervals on a cooled CCD Hammamatsu camera shuttered at 0.5 s.

References

1. Vithalani KK, De Shoffner JD, Lozanne A. Isolation and characterization of a novel cytokinesis-deficient mutant in *Dictyostelium discoideum*. J Cell Biochem 1996;62:290–301.
2. Kwak E, Gerald N, Larochelle DA, Vithalani KK, Niswonger ML, De Maready M, Lozanne A. LvsA, a protein related to the mouse beige protein, is required for cytokinesis in *Dictyostelium*. Mol Biol Cell 1999;10:4429–4439.
3. Nagle DL, Karim MA, Woolf EA, Holmgren L, Bork P, Misumi DJ, McGrail SH, Dussault BJ, Perou CM, Boissy RE, Duyk GM, Spritz RA, Moore KJ. Identification and mutation analysis of the complete gene for Chediak–Higashi syndrome. Nat Genet 1996;14:307–311.
4. McVey Ward D, Griffiths GM, Stinchcombe JC, Kaplan J. Analysis of the lysosomal storage disease Chediak–Higashi syndrome. Traffic 2000;1:816–822.
5. Burkhardt JK, Wiebel FA, Hester S, Argon Y. The giant organelles in beige and Chediak–Higashi fibroblasts are derived from late endosomes and mature lysosomes. J Exp Med 1993;178:1845–1856.
6. Adam-Klages S, Adam D, Weigmann K, Struve S, Kolanus W, Schneider-Mergener J, Kronke M. FAN, a novel WD-repeat protein, couples the p55 TNF-receptor to neutral sphingomyelinase. Cell 1996;86:937–947.
7. O'Halloran TJ. Membrane traffic and cytokinesis. Traffic 2000;1:921–926.
8. Niswonger ML, O'Halloran TJ. A novel role for clathrin in cytokinesis. Proc Natl Acad Sci USA 1997;94:8575–8578.
9. Gerald N, Damer CK, De O'Halloran TJ, Lozanne A. Cytokinesis failure in clathrin-minus cells is caused by cleavage furrow instability. Cell Motil Cytoskeleton 2001;48:213–223.
10. Wang X, Herberg FW, Laue MM, Wullner C, Hu B, Petrasch-Parwez E, Kilimann MW. Neurobeachin: a protein kinase A-anchoring, beige/Chediak–Higashi protein homolog implicated in neuronal membrane traffic. J Neurosci 2000;20:8551–8565.
11. Wang JW, Howson J, Haller E, Kerr WG. Identification of a novel lipopolysaccharide-inducible gene with key features of both A kinase anchor proteins and chs1/beige proteins. J Immunol 2001;166:4586–4595.
12. Heuser J, Zhu Q, Clarke M. Proton pumps populate the contractile vacuoles of *Dictyostelium* amoebae. J Cell Biol 1993;121:1311–1327.

13. Liu T, Clarke M. The vacuolar proton pump of *Dictyostelium discoideum*: molecular cloning and analysis of the 100 kDa subunit. J Cell Sci 1996;109:1041–1051.

14. Zhu Q, Liu T, Clarke M. Calmodulin and the contractile vacuole complex in mitotic cells of *Dictyostelium discoideum*. J Cell Sci 1993;104:1119–1127.

15. Becker M, Matzner M, Gerisch G. Drainin required for membrane fusion of the contractile vacuole in *Dictyostelium* is the prototype of a protein family also represented in man. EMBO J 1999;18:3305–3316.

16. Zhu Q, Clarke M. Association of calmodulin and an unconventional myosin with the contractile vacuole complex of *Dictyostelium discoideum*. J Cell Biol 1992;118:347–358.

17. Gabriel D, Hacker U, Kohler J, Muller-Taubenberger A, Schwartz JM, Westphal M, Gerisch G. The contractile vacuole network of *Dictyostelium* as a distinct organelle: its dynamics visualized by a GFP marker protein. J Cell Sci 1999;112:3995–4005.

18. Bush J, Temesvari L, Rodriguez-Paris J, Buczynski G, Cardelli J. A role for a Rab4-like GTPase in endocytosis and in regulation of contractile vacuole structure and function in *Dictyostelium discoideum*. Mol Biol Cell 1996;7:1623–1638.

19. Ruscetti T, Cardelli JA, Niswonger ML, O'Halloran TJ. Clathrin heavy chain functions in sorting and secretion of lysosomal enzymes in *Dictyostelium discoideum*. J Cell Biol 1994;126:343–352.

20. Doberstein SK, Baines IC, Wiegand G, Korn ED, Pollard TD. Inhibition of contractile vacuole function *in vivo* by antibodies against myosin-I. Nature 1993;365:841–843.

21. Temesvari LA, Bush JM, Peterson MD, Novak KD, Titus MA, Cardelli JA. Examination of the endosomal and lysosomal pathways in *Dictyostelium discoideum* myosin I mutants. J Cell Sci 1996;109:663–673.

22. Tani T, Allen RD, Naitoh Y. Cellular membranes that undergo cyclic changes in tension. Direct measurement of force generation by an *in vitro* contractile vacuole of *Paramecium multimicronucleatum*. J Cell Sci 2001;114:785–795.

23. Döbereiner H-G, Selchow O, Lipowsky R. Spontaneous curvature of fluid vesicles induced by trans-bilayer sugar asymmetry. Eur Biophys J 1999;28:174–178.

24. Zha X, Pierini LM, Leopold PL, Skiba PJ, Tabas I, Maxfield FR. Sphingo-myelinase treatment induces ATP-independent endocytosis. J Cell Biol 1998;140:39–47.

25. Damer CK, O'Halloran TJ. Spatially regulated recruitment of clathrin to the plasma membrane during capping and cell translocation. Mol Biol Cell 2000;11:2151–2159.

26. Fukui Y, Inoue S. Cell division in *Dictyostelium* with special emphasis on actomyosin organization in cytokinesis. [published erratum appears in Cell Motil Cytoskeleton 1991;19(4):290] Cell Motil Cytoskeleton 1991;18:41–54.

27. Liu T, Williams JG, Clarke M. Inducible expression of calmodulin antisense RNA in *Dictyostelium* cells inhibits the completion of cytokinesis. Mol Biol Cell 1992;3:1403–1413.

28. Li CJ, Heim R, Lu P, Pu Y, Tsien RY, Chang DC. Dynamic redistribution of calmodulin in HeLa cells during cell division as revealed by a GFP-calmodulin fusion protein technique. J Cell Sci 1999;112:1567–1577.

29. Fluck RA, Miller AL, Jaffe LF. Slow calcium waves accompany cytokinesis in Medaka fish eggs. J Cell Biol 1991;115:1259–1265.

30. Miller AL, Fluck RA, McLaughlin JA, Jaffe LF. Calcium buffer injections inhibit cytokinesis in Xenopus eggs. J Cell Sci 1993;106:523–534.

31. Sussman M. Cultivation and synchronous morphogenesis of *Dictyostelium* under controlled experimental conditions. In: Spudich JA, editor. Dictyostelium Discoideum: Molecular Approaches to Cell Biology. New York: Academic Press, Inc; 1987. p. 9–29.

32. Moores SL, Sabry JH, Spudich JA. Myosin dynamics in live *Dictyostelium* cells. Proc Natl Acad Sci USA 1996;93:443–446.

33. De Lozanne A, Spudich JA. Disruption of the *Dictyostelium* myosin heavy chain gene by homologous recombination. Science 1987;236:1086–1091.

34. Koonce MP, McIntosh JR. Identification and immunolocalization of cytoplasmic dynein in *Dictyostelium*. Cell Motil Cytoskeleton 1990;15:51–62.

35. Seedorf M, Damelin M, Kahana J, Taura T, Silver PA. Interactions between a nuclear transporter and a subset of nuclear pore complex proteins depend on Ran GTPase. Mol Cell Biol 1999;19:1547–1557.

36. Fok AK, Clarke M, Ma L, Allen RD. Vacuolar H (+) -ATPase of *Dictyostelium discoideum*. A monoclonal antibody study. J Cell Sci 1993;106:1103–1113.